10.1109/ULTSYM.2015.0426

Velocity Vector in three dimensions using a high-frame-rate dual-transducer setup

Richard Rau[¶], Pieter Kruizinga[*‡], Hendrik J. Vos[*‡], Wolfgang Scheffer [¶], Johannes G Bosch[*], Georg Maret [¶], Antonius F.W. van der Steen[*†‡§] and Nico de Jong[*†‡]

[*]Thorax Center, Erasmus MC, Rotterdam, The Netherlands
[†]Interuniversity Cardiology Institute, Utrecht, The Netherlands
[‡]Delft University of Technology, Delft, The Netherlands
[§]Shenzhen Institutes of Advanced Technology, Chinese Academy of Sciences, Shenzhen, China
[¶]Department of Physics, Universität Konstanz, Konstanz, Germany

***Abstract*—High-frame-rate ultrasound imaging has great potential to improve conventional Doppler imaging because large ensemble acquisitions are available for every pixel in an image. Additionally it allows deriving the lateral motion using angled plane-wave beams. Despite its clinical success, conventional Doppler techniques remain limited due to the inability to measure out-of-plane flow. In this paper we present a solution for measuring all flow directions by using two linear array transducers with overlapping beams. By triangulation of the 2D Doppler signals derived for the individual imaging planes we derive the full 3D velocity vector. We show experimental proof that this imaging setup allows to extract the 3D velocity vector of blood in a human carotid artery.**

I. Introduction

The carotid arteries (CAs) supply the brain with oxygenated blood. When these arteries are affected by atherosclerosis, which causes plaques to grow inside the artery wall, the blood flow may be compromised. When these plaques cause narrowing of the lumen, the peak systolic velocity of the blood flow around and in this stenotic region will change. The measure of this velocity seems to be an important indication in the clinical evaluation of carotid stenosis [1]. The blood flow velocity inside the CA can be measured noninvasively using ultrasound Doppler (USD). In the recent years progress has been made to further increase the reproducibility and sensitivity of USD. A major improvement in terms of sensitivity has been accomplished by the application of high-frame-rate (HFR) imaging. With this HFR technique limited diffraction beams are used to insonify the medium at once and image reconstruction is accomplished after receiving the echoes [2, 3]. This technique ensures an adequate sampling of the possible flow velocities in the entire field of view.

Despite the success of USD as a major clinical tool, the difficulty of measuring true user-independent blood flow velocities is still a challenging problem. This problem is mainly due to the fact that Doppler signals are normally acquired within a 2D imaging plane whereas the flow velocity vector is intrinsically 3D. The third component of the flow velocity vector that cannot be measured directly, named the out-of-plane motion, contaminates the velocity estimation in the 2D plane. This especially happens around large stenotic lesions and around the bifurcation in the CA where the flow can be very complex.

Possibly the best method for measuring the full 3D velocity field is using a 2D array which would enable full 3D HFR imaging [4]. However these arrays are not abundantly available, especially not for carotid imaging, and the scanners that could deal with these high volume rates are also not yet available for clinical use. One of the best attempts proposed to address the out-of-plane motion problem using conventional linear arrays, is the technique of intrinsic spectral broadening [5–7]. The main principle underlying this technique is the correction of the received Doppler spectrum (shape) with an estimated or predicted spectrum. The reasoning here is that out-of-plane motion causes the spectrum to broaden with respect to the predicted spectrum. Obviously this technique relies strongly on the characterization of the estimated spectrum. When for instance the flow becomes complex and cannot be modelled a priori, these methods fail.

In this paper we explore a new and robust method for deriving the 3D velocity vector field using two conventional linear arrays that are connected to a commercially available ultrasound machine. The two arrays are joined in such a manner that the imaging planes intersect under a 45 degree angle inside the CA lumen.

For each imaging plane we obtain a 2D velocity vector field using tilted plane-wave transmissions and conventional triangulation of the received Doppler signals [3]. The two, 2D velocity vector fields are then combined to obtain the 3D velocity vector field using again triangulation between the different angled observations. Figure 1 shows a schematic representation of the proposed dual-transducer Doppler method. We tested this new imaging method comprising two linear arrays on a healthy volunteer and we show experimental proof that this setup allows us to extract the 3D velocity

978-1-4799-8182-3/15/$31.00 ©2015 IEEE

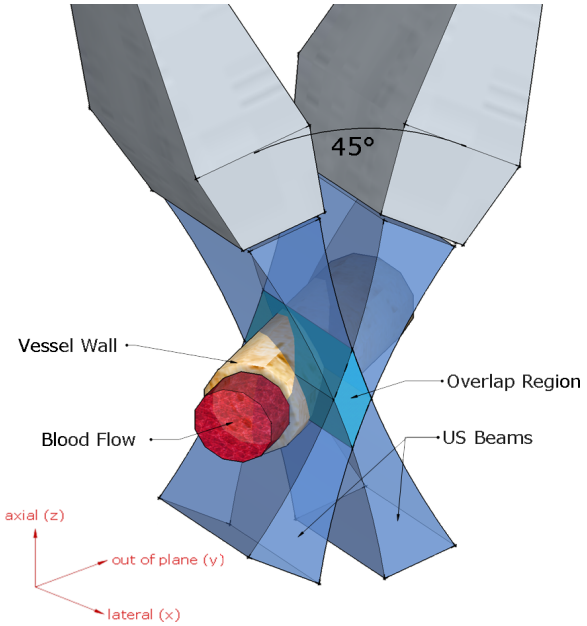

Fig. 1: Experimental setup with two transducers scanning the carotid artery at an angle arrangement of 45°. The overlap of two plane wave emissions (transparent blue) is shown to be in the region of the carotid artery.

vector of blood in a human carotid artery.

II. Methods

To show the proof of concept of this dual-transducer method we used two relatively low-frequency linear array transducers (ATL L7-4, 5MHz). A custom made holder kept the transducers at a 45 degree angle. The transducers were connected to a commercial ultrasound research system (Vantage 256Tx/256Rx, Verasonics). The Verasonics system has two active connectors and allows two transducers to be connected and accessed at the same time. The interleaved Doppler acquisitions for both transducers involved an ensemble length of 150, three angled plane-wave beams (-7, 0, + 7 degree) and a Doppler pulse repetition rate of 2.5kHz at a 5MHz transmission frequency (2.5 cycle Gaussian modulated). After clutter rejection the velocity signal was derived for the three angled beams of each transducer with the first lag autocorrelation. The lateral and axial flow components were derived by triangulation as described in [3]. Using the dual-transducer method an additional triangulation step for the out-of-plane axis can be performed in the overlap region. The overlap region (light-blue region in Fig.1) can be confirmed by measuring the Doppler signal of the CA, using one transducer in transmit and both in receive mode. If the blood flow in the lumen is imaged well for both transducers, it is justified to triangulate the signal along the out-of-plane axis, given that a homogeneous flow profile is abundant. This is verified in Fig. 2, where it can be seen that the spatial dimensions and magnitude of the measured Power Doppler signal are the same for both transducers. If - for the non-transmitting transducer - only a limited region within the CA results in Doppler signal, the data could only

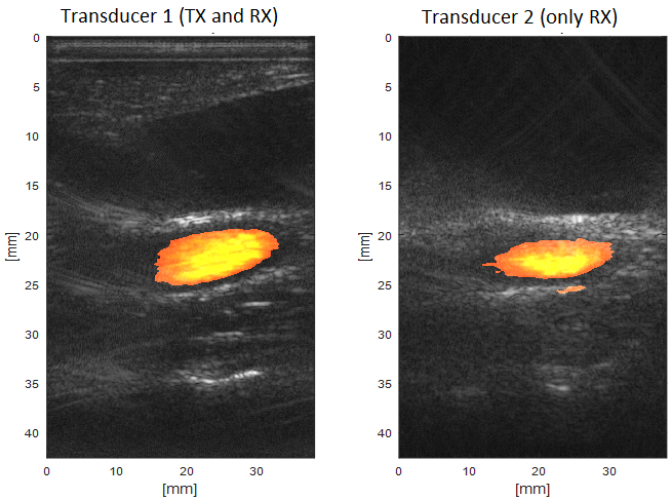

Fig. 2: Combined gray-scale and Doppler images showing the received (RX) Power Doppler signal of both transducers when only one transducer is transmitting (TX).

be triangulated in this limited region. As the Doppler signal in Fig. 2 shows the same lumen sizing for both transducers, the out-of-plane triangulation is justified within whole lumen.

In order to quantify the 3D blood flow velocities with lateral (x), out-of-plane (y) and axial (z) components, it can be derived that

$$v^{(x)}_{n,m} = \frac{c}{8f_0 \sin(\theta_{n,m})}\left[(\hat{f}^{(1)}_n - \hat{f}^{(1)}_m) + (\hat{f}^{(2)}_n - \hat{f}^{(2)}_m)\right] \quad (1)$$

$$v^{(y)}_{n,m} = \frac{c}{8f_0 \cos(\theta_{n,m})\sin(\phi)}\left[(\hat{f}^{(1)}_n + \hat{f}^{(1)}_m) + (\hat{f}^{(2)}_n + \hat{f}^{(2)}_m)\right] \quad (2)$$

$$v^{(z)}_{n,m} = \frac{c}{8f_0 \cos(\theta_{n,m})\cos(\phi)}\left[(\hat{f}^{(1)}_n + \hat{f}^{(1)}_m) + (\hat{f}^{(2)}_n + \hat{f}^{(2)}_m)\right] \quad (3)$$

where f_0 is the center frequency of the transmitted pulse and $f^i_{n,m}$ is the Doppler shifted frequency of transducer i with n or m being the corresponding angled plane-wave transmission of each transducer. $\phi = 22.5°$ is the half angle opening of the angled transducer setup and $\theta_{n,m} = (\theta_n - \theta_m)/2$ the half angle opening of two triangulated angled beams for each transducer with $n \neq m$. The overall velocity is then averaged over all calculations to

$$v^{(i)} = \frac{2}{N_a(N_a-1)} \sum_{1 \leq n < m \leq N_a} v^{(i)}_{n,m} \quad (4)$$

for all components $i = [x, y, z]$ with N_a=3 being the number of angled beams for each transducer.

III. Results

The results of the dual-transducer velocity estimation setup for a carotid artery measurement are shown in Figs. 3 and 4. In Fig 3 we show the B-Mode images of the two transducers as well as the overlaid velocity vectors in three dimensions. The region of interest is marked purple in the image and shown in detailed 2D color Doppler maps in Fig. 4 for all separate velocity components. The velocity in the lumen center is estimated to be $v = (-31 \pm 1 \;//\; 725 \pm 34 \;//\; -299 \pm 8)\ mm/s$ in axial, lateral and out-of-plane direction, respectively, in

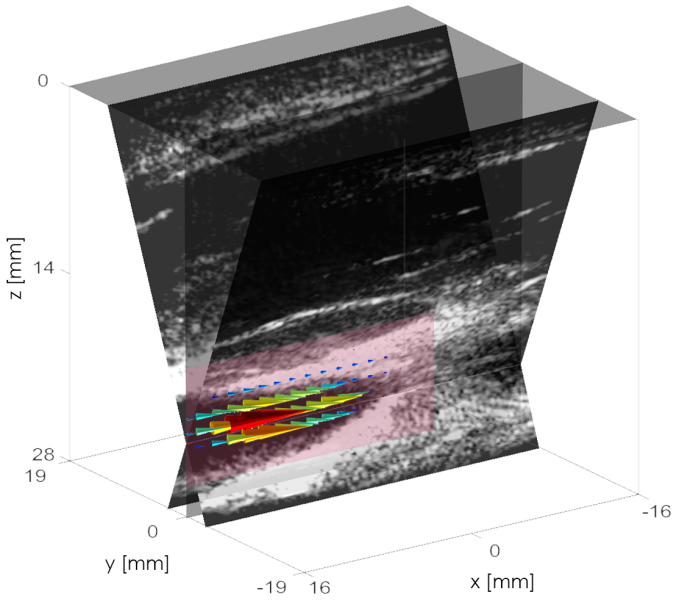

Fig. 3: B-mode images of the two transducers, superimposed by the 3D velocity vector cones in the beam overlap region (purple overlay). The cone colors indicate the magnitude of the velocity component

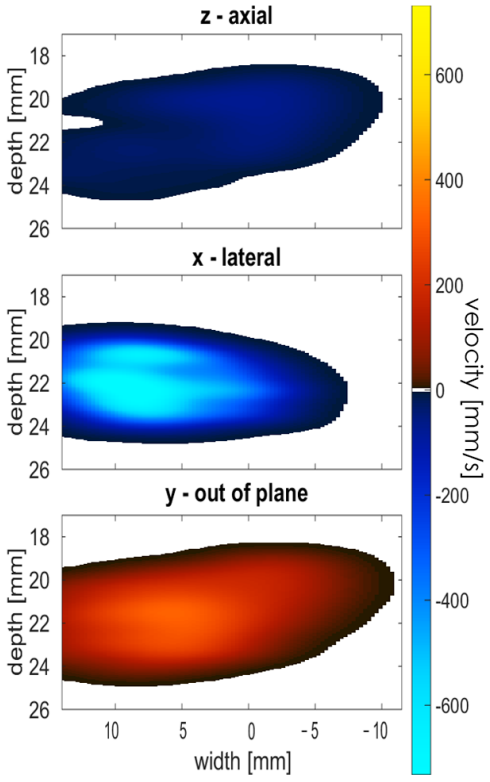

Fig. 4: Velocity maps of the three separate components in the overlap region (marked in purple in fig. 3).

which the uncertainty is derived by the 2D standard deviation of the 75 pixels in the lumen center, which resembles an approximate area of $(1.5mm)^2$. These values yield a RMS absolute flow velocity of $785 \pm 53mm/s$, which is mainly oriented in the lateral (x) direction.

IV. Discussion and Concluding remarks

We showed the determination of blood flow velocities in all three dimensions with a simple setup of two transducers. Compared to other recent 3D vector flow measurement techniques, which require complicated matrix array transducers, our method can be accomplished with only two conventional linear array transducers and still results in robust data for in vivo measurements.

One limitation of this technique is that the imaging area is restricted by the overlap of the fixed foci of the two transducers. This results in two problems, a limited depth range and a finite sizing of the sample volume. The limitation of depth range can be overcome dynamically for example by wobbling one transducer and thereby moving the sample volume in depth along the other transducer beam or statically by decreasing the separation distance as well as the angle ϕ between the two transducers. The latter solution would stretch the sample volume in axial direction, however with the drawback that the out-of-plane triangulation becomes more error prone, because of the inverse proportionality of $\sin(\phi)$ in the out-of-plane velocity estimation (see eq. (2)). The best method to tackle the depth range problem still needs to be evaluated in future experiments.

For the proposed dual-transducer setup we assume homogeneous flow inside the overlap region in order to justify the triangulation of the two transducer beams. This assumption can be challenged in real-life situations. Further study is ongoing to see whether the straightforward triangulation can be adapted to account for inhomogeneous flow inside the overlap region. One such advancement could be to correct the received spectrum for as proposed in the spectral broadening correction techniques [6, 7]. The benefit of having two identical transducers sampling the same volume under different angles may just provide the information needed to provide a unique solution to correct for the spectral broadening.

For future experiments in the dual-transducer setup we first aim to quantify the limitation of the elevational resolution in more detail by defining the sample volume size in dependence of angle and separation distance between the transducers. This will help to derive the best set of parameters in absence of complex flow profiles. Furthermore, phantom measurement should provide a better understanding of the influence of complex flow inside the overlap region.

In conclusion, we provided proof that 3D flow fields with realistic flow velocities inside the CA can be measured in-vivo using a simple setup of two conventional linear array transducers.

References

[1] E. G. Grant, C. B. Benson, G. L. Moneta, A. V. Alexandrov, J. D. Baker, E. I. Bluth, B. A. Carroll, M. Eliasziw,

J. Gocke, B. S. Hertzberg *et al.*, "Carotid artery stenosis: Gray-scale and doppler us diagnosis - society of radiologists in ultrasound consensus conference1," *Radiology*, 2003.

[2] M. Tanter, J. Bercoff, L. Sandrin, and M. Fink, "Ultrafast compound imaging for 2-d motion vector estimation: application to transient elastography," *Ultrasonics, Ferroelectrics and Frequency Control, IEEE Transactions on*, vol. 49, no. 10, pp. 1363–1374, 2002.

[3] I. Ekroll, A. Swillens, P. Segers, T. Dahl, H. Torp, and L. Lovstakken, "Simultaneous quantification of flow and tissue velocities based on multi-angle plane wave imaging," *Ultrasonics, Ferroelectrics and Frequency Control, IEEE Transactions on*, vol. 60, no. 4, pp. 727–738, 2013.

[4] J. Provost, C. Papadacci, C. Demene, J.-L. Gennisson, M. Tanter, and M. Pernot, "3-d ultrafast doppler imaging applied to the noninvasive mapping of blood vessels in vivo," *Ultrasonics, Ferroelectrics, and Frequency Control, IEEE Transactions on*, vol. 62, no. 8, pp. 1467–1472, August 2015.

[5] V. Newhouse, D. Censor, T. Vontz, J. A. Cisneros, and B. B. Goldberg, "Ultrasound doppler probing of flows transverse with respect to beam axis," *Biomedical Engineering, IEEE Transactions on*, vol. BME-34, no. 10, pp. 779–789, Oct 1987.

[6] P. Tortoli, L. Bessi, and F. Guidi, "Bidirectional doppler signal analysis based on a single rf sampling channel," *Ultrasonics, Ferroelectrics, and Frequency Control, IEEE Transactions on*, vol. 41, no. 1, pp. 1–3, Jan 1994.

[7] B.-F. Osmanski, G. Montaldo, and M. Tanter, "Out-of-plane doppler imaging based on ultrafast plane wave imaging," *Ultrasonics, Ferroelectrics, and Frequency Control, IEEE Transactions on*, vol. 62, no. 4, pp. 625–636, April 2015.